http://ansinet.com/itj

ITJ

ISSN 1812-5638

INFORMATION TECHNOLOGY JOURNAL

ANSInet
Asian Network for Scientific Information
308 Lasani Town, Sargodha Road, Faisalabad - Pakistan

Information Technology Journal 12 (18): 4508-4512, 2013
ISSN 1812-5638 / DOI: 10.3923/itj.2013.4508.4512

Numerical Simulation of Orifice Plate's Backflow Region Characteristics

Ai Wan-Zheng and Pan Li-Ping
School of Navigation, Zhejiang Ocean University, Zhoushan, 316021, Zhejiang, China

Abstract: The backflow region length of orifice plate, relating directly to the energy dissipation ratio and the setting of multi-stage orifice plates, is an important index of those energy dissipaters. In the present study, this coefficient and relative parameters were analyzed by theoretical considerations and their relationships were obtained by the numerical simulations. It could be concluded that the backflow region length was mainly dominated by the contraction ratio of the orifice plate as well as the ratio of the orifice plate thickness to tunnel's diameter. The less the contraction ratio of the orifice plate is, the larger is the backflow region length. When Reynolds number is more than 10^5, Reynolds number has little impact on backflow region length. The conclusions obtained in this study can provide references for setting the distance between two orifice plates in installing multi-stage orifice plates.

Key words: Backflow region, contraction ratio, head loss coefficient, orifice plate, thickness

INTRODUCTION

In terms of a high dam project, the energy dissipation for flood discharges is an important problem that affects the safety of this project directly. With the development of hydropower projects, the heights of some dams have got to and exceeded the level of 300 m, such as 305 and 315 m for the Jinping first-cascade hydropower project and the Shuangjiangkou hydropower project in Sichuan province, respectively. Over 30 hydropower projects with the height of over 100 m have been completed or under constructions since 2000 in China (Zhou *et al*., 2006). The energy dissipation for most of the high dam projects is characterized by deep valley, high water head and large discharge (Zhang *et al*., 1991; Lin, 1985). The power of the flood discharge, like the Xiluodu hydropower project in China with about 100 million kW, gets to the biggest one in the world. As a kind of energy dissipators with sudden reduction and sudden enlargement forms, multi-orifice plates, have been used in the hydropower projects due to its simple structure, convenient construction and high energy dissipation ratio. A typical application for multi-stage orifice plates is in Xiao Lang Di Hydropower Projects on the Yellow River, china. Three sharp-edged orifice plates were installed in discharge tunnel in this project, getting the energy dissipation ratio of about 44% (Wu *et al*., 1995).

The flow through an orifice plate is shown in Fig. 1. There exist the vortex regions of ring form after the orifice plate due to the sudden reduction and sudden enlargement of the orifice plate and those vortices are the original regions of the energy dissipation. L_b in Fig. 1 is the length of backflow region. Many of researches about the orifice plate have been conducted, in which the energy dissipation and the cavitations are the two main items. Those two problems are all mainly related to the contraction ratio of the orifice plate, the smaller the contraction ratio is, the larger orifice plate's head loss coefficient and incipient cavitations number are (Ball *et al*., 1975; Ai and Ding, 2010). However, the length of backflow region after orifice plate is an important parameter, not only it is closely related with orifice plate's energy dissipation efficiency, but also it is a valuable reference parameter when designing the distance between two orifice plates in multi-stage orifice plates. If the distance between two orifice plates is shorter than the length of backflow region, flow's regime does not recover fully and the function of orifice plate's energy dissipation will be weakened (He and Zhao, 2010). With respect to the length of orifice plate's backflow region, (Wang and Yue, 1987) regarded that the length of orifice plate's backflow

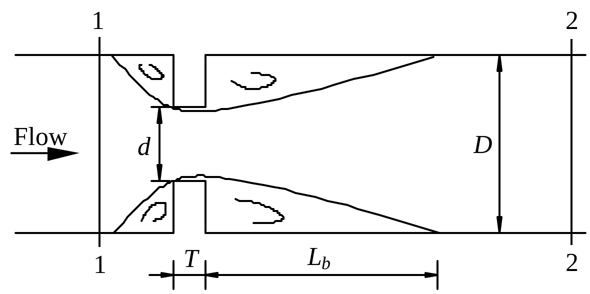

Fig. 1: Flow through orifice plate

Corresponding Author: Ai Wan-Zheng, School of Navigation, Zhejiang ocean University, Zhoushan, 316021, Zhejiang, China

region is closely related with contraction ratio, the smaller the contraction ratio is, the longer the length of orifice plate's backflow region is (Wang and Yue, 1987). Zhao (1993) deemed that flows can recover normally if the distance between two orifice plates in multi-stage orifice plates is more than 3D (D is tunnel's diameter), so it is feasible to arrange 3D spacing between two orifice plates in multi-stage orifice plates. However, Zhao's research did not embody the impacts of contraction ratio and backflow region length on the distance between orifice plates. As a matter of fact, besides contraction ratio, the other parameters' effects on the length of backflow region performances are also remarkable, such as the hydraulic parameters including flow's velocity and flow's dynamic viscosity which stand for the state of flow; such as geometric parameter, the orifice plate thickness (T in Fig. 1), because of the orifice plate thickness can affect flow's sudden reduction and sudden enlargement (Wu *et al.*, 2010). The purposes of the present work, therefore, are to investigate the effects of the geometric and hydraulic parameters, i.e., the contraction ratio and the ratio of the orifice plate thickness et, on the backflow region length; and to present an empirical expression of the backflow region length to both the contraction ratio and the dimensionless thickness of the orifice plate, by means of the numerical simulations.

THEORETICAL CONSIDERS

There are many parameters which affect the backflow region length after an orifice plate and the relevant parameters of dimensional analysis come from the following groups:

- **Fluid properties:** These consist of: the density of water ρ (kg m^{-3}), the dynamic viscosity of water μ (N.s m^{-2})
- **Tunnel and orifice plate energy dissipater geometry:** They are: The tunnel diameter D (m), the orifice diameter d (m) and the orifice plate thickness T (m). Let the contraction ratio of the orifice plate diameter and the tunnel diameter as β = d/D, the ratio of the orifice plate thickness to the tunnel diameter as α = T/D and the ratio of backflow region length to the tunnel diameter as $l_b=L_b/D$
- **Flow property:** It is mainly refers to the average flow velocity in tunnel u (m sec^{-1})

Each of these design parameters is a function of the initial independent parameters:

$$L_b = f(\rho, \mu, D, d, T, u) \quad (1)$$

This relationship could be rewritten in terms of dimensionless parameters:

$$L_b/D = f(d/D, T/D, uD\rho/\mu) \quad (2)$$

That is:

$$l_b = f(\beta, a, R_e) \quad (3)$$

where, Re is Reynolds number. That implies that the dimensionless backflow region length l_b is the function of β, α and Re. The study procedure was outlined considering variable parameters in dimensionless backflow region length in Eq. 3 in order to find out the effects of each parameter independently on it.

NUMERICAL SIMULATION

Numerical simulations model: The RNG k~ε model was used to calculate the hydraulic parameters of the flow through the orifice plate, due to its suitability for simulating the flow inside large change boundary forms as well as its high precision and calculation stability. For the steady and incompressible flows, the governing equations of this model can be written as (Yang and Zhao, 1992).

Continuity equation:

$$\frac{\partial u_i}{\partial x_i} = 0 \quad i = 1, 2 \quad (4)$$

Momentum equation:

$$u_j \frac{\partial u_i}{\partial x_j} = -\frac{1}{\rho}\frac{\partial p}{\partial x_i} + \frac{\partial}{\partial x_j}[(\nu + \nu_t)(\frac{\partial u_i}{\partial x_j} + \frac{\partial u_j}{\partial x_i})] \quad i = 1, 2 \quad (5)$$

k-equation:

$$u_i \frac{\partial k}{\partial x_i} = \frac{\partial}{\partial x_j}\left[\alpha_k(\nu + \nu_t)\frac{\partial k}{\partial x_j}\right] + \frac{1}{\rho}G_k - \varepsilon \quad i = 1, 2 \quad (6)$$

ε-equation:

$$u_i \frac{\partial \varepsilon}{\partial x_i} = \frac{\partial}{\partial x_j}\left[\alpha_\varepsilon(\nu + \nu_t)\frac{\partial \varepsilon}{\partial x_j}\right] + \frac{1}{\rho}C_1^* G_k \frac{\varepsilon}{k} - C_2\frac{\varepsilon^2}{k} \quad i = 1, 2 \quad (7)$$

where, x_i (= x, y) are the coordinates in longitudinal and transverse directions, respectively; u_i (= u_x, u_y) are the velocity components in x and y directions, respectively; ρ is the density of water; p is the pressure; ν is the kinematics viscosity; ν_t is the eddy viscosity and can be given by $\nu_t = C_\mu(k^2/\varepsilon)$, in which k is the turbulence kinetic energy, ε is the dissipation rate of k and C_μ = 0.085. The other parameters are:

$$C_1^* = C_1 - \frac{\eta(1-\eta/\eta_0)}{1+\lambda\eta^3},\ \eta = Sk/\varepsilon,\ S = \frac{1}{2}\left(\frac{\partial u_i}{\partial x_j} + \frac{\partial u_j}{\partial x_i}\right)$$

$$C_1 = 1.42,\ \eta_o = 4.377,\ \lambda = 0.012,\ G_k = \rho v_t\left(\frac{\partial u_i}{\partial x_j} + \frac{\partial u_j}{\partial x_i}\right)\frac{\partial u_i}{\partial x_j}$$

$$C_2 = 1.68 \text{ and } \alpha_k = \alpha_c = 1.39$$

The calculation boundary conditions are treated as follows: In the inflow boundary the turbulent kinetic energy k_{in} and the turbulent dissipation rate ε_{in} can be defined as respectively:

$$k_{in} = 0.0144u_{in}^2,\ \varepsilon_{in} = \frac{k_{in}^{1.5}}{(0.25D)} \qquad (8)$$

where, u_{in} is the average velocity in the inflow boundary. In the outflow boundary the flow is considered as developed fully. The wall boundary is controlled by the wall functions (Xia and Ni, 2003). And the symmetric boundary condition is adopted that is, the radial velocity on symmetry axis is zero.

Numerical simulations phases: Two kinds of calculation phases were simulated and these phases are: Phase No.1, to calculate the dimensionless backflow region length l_b at the range of Reynolds number $R = 9.00\times10^4$-2.76×10^6 when $\beta = 0.50$ and $\alpha = 0.10$, in order to analysis the effects of Re on l_b. Phase No. 2, to calculate orifice plate head loss coefficient ξ and the dimensionless backflow region length l_b at the different β and α when $R = 1.80\times10^5$, to discuss the relationship between ξ and l_b, to discuss the variations of the dimensionless backflow region length l_b with β and α and to establish the relationship expression of them. Orifice plate head loss coefficient ξ is defined as the following:

$$\xi = \frac{p_1 - p_2}{0.5\rho u^2} \qquad (9)$$

where, p_1 is the average pressure at sections 1-1 (shown in Fig 1) which is located in the position of 0.5D before the orifice plate; p_2 is the average pressure at sections 2-2 (shown in Fig 2) which is located in the position of 3.0 D after the orifice plate. u is the average flow velocity in tunnel.

The diameter (D) of the tunnel is 0.21 m. The range of the numerical simulations was selected at 6.0 D before the orifice plate at the beginning and at 6.0 D after the orifice plate at the end. The method to determine backflow region length is as the following: taking a section along tunnel direction which is very close to the tunnel's wall; viewing the flow's horizontal velocity at this section; regarding the distance between orifice plate rear and the point, where flow's horizontal velocity is 0, is backflow region length.

Numerical simulation results: Figure 2 and 3 are the streamlines when $\beta = 0.4$, but $\alpha = 0.05$ and $\alpha = 0.5$, respectively. From the two figures, it can be learned that there exists large backflow region after orifice plate.

Numerical simulation results are shown in Table 1 and 2, respectively.

Table 1: Variations of l_b with Re ($\beta = 0.50$, $\alpha = 0.10$)

R ($\times10^5$)	0.90	1.80	9.20	18.40	27.60
l_b	3.14	3.15	3.15	3.15	3.15

Table 2: Variations of l_b and ξ with β and α (Re = 1.8×10^5)

	α				
β	0.05	0.10	0.15	0.20	0.25
0.40	$l_b = 3.50$	$l_b = 3.40$	$l_b = 3.22$	$l_b = 3.15$	$l_b = 3.07$
	$\xi = 93.00$	$\xi = 92.00$	$\xi = 85.50$	$\xi = 78.50$	$\xi = 74.30$
0.50	$l_b = 3.26$	$l_b = 3.15$	$l_b = 2.98$	$l_b = 2.89$	$l_b = 2.79$
	$\xi = 31.70$	$\xi = 31.20$	$\xi = 29.40$	$\xi = 27.80$	$\xi = 26.30$
0.60	$l_b = 2.69$	$l_b = 2.61$	$l_b = 2.44$	$l_b = 2.34$	$l_b = 2.24$
	$\xi = 12.30$	$\xi = 12.20$	$\xi = 11.50$	$\xi = 11.00$	$\xi = 10.30$
0.70	$l_b = 1.95$	$l_b = 1.92$	$l_b = 1.78$	$l_b = 1.69$	$l_b = 1.58$
	$\xi = 4.30$	$\xi = 4.20$	$\xi = 3.80$	$\xi = 3.60$	$\xi = 3.20$
0.80	$l_b = 1.21$	$l_b = 1.20$	$l_b = 1.11$	$l_b = 1.01$	$l_b = 0.91$
	$\xi = 1.50$	$\xi = 1.50$	$\xi = 1.40$	$\xi = 1.30$	$\xi = 1.20$

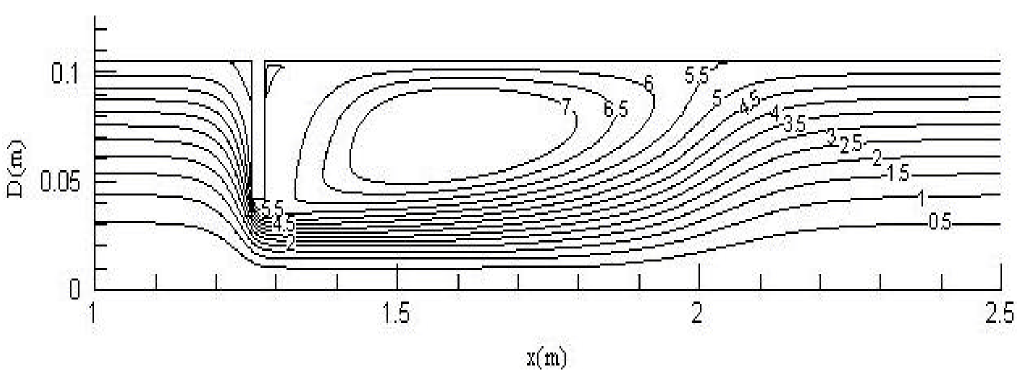

Fig. 2: Streamline ($\beta = 0.4$, $\alpha = 0.05$)

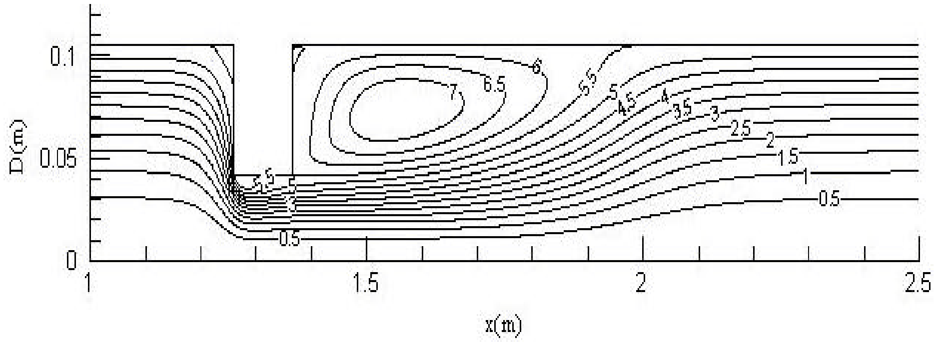

Fig. 3: Streamline ($\beta = 0.4$, $\alpha = 0.5$)

DISCUSSION

Relation between backflow region length and reynolds number: Figure 4 is the numerical simulation results of the dimensionless backflow region length after the orifice plate l_b and Reynolds number Re which derives from the data in Table 1. It could be seen that the dimensionless backflow region lengths l_b have hardly changes with Reynolds number Re approximately. And they changed from 3.14-3.15, respectively with regard to the changes of Reynolds number Re from 9.00×10^4 to 2.76×10^6. Therefore it could be concluded that the effects of Reynolds number Re could be neglected on the dimensionless backflow region length l_b in the considered range of Re that is to say, l_b is only the function of the geometric parameters of the orifice plate, i.e., β and α.

Relation between backflow region length and energy dissipation: Figure 5 shows the effects of the backflow region length lb on the head loss coefficient ξ which was drawn by means of the data in Table 2. It is can be concluded that the longer the backflow region length is, the larger is head loss coefficient which illustrates that backflow region is an important source of energy dissipation for orifice plate. The main reason for this phenomenon is that the longer the length of backflow region is, the greater is the scope of vortex of the backflow region after the orifice plate, where there are the intensive shear stress and intensive friction actions of the flow.

Characteristics of backflow region length: Figure 6 is drawn by using the data in Table 2 which embodies the relationships between l_b and the geometric parameters of the orifice plate. Figure 4 shows that l_b decreases with the increasing of β when a is constancy; l_b decreases also with the increasing of a when β is constancy. In a word, the dimensionless backflow region length l_b is essentially controlled by the contraction ratio β and dimensionless

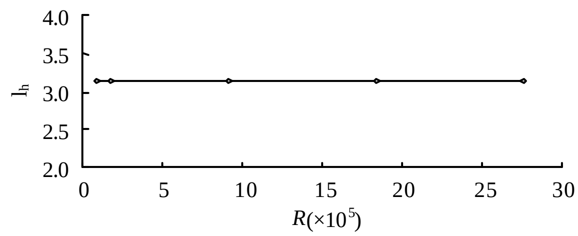

Fig. 4: Variations of l_b with reynolds number

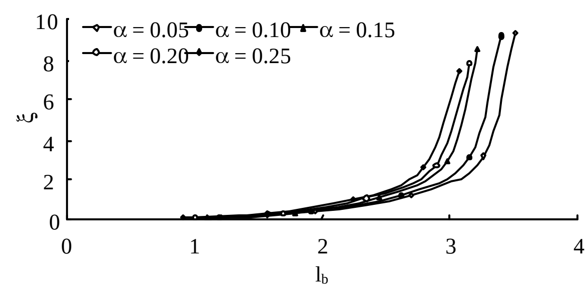

Fig. 5: Relationship between l_b and ξ

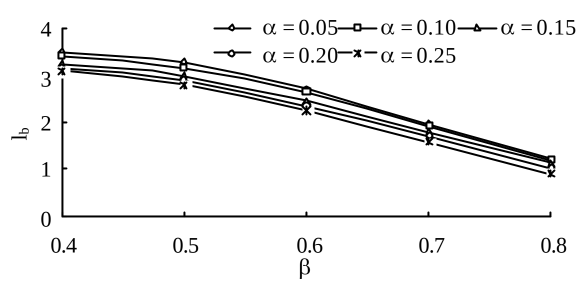

Fig. 6: Variations of l_b with β, a

thickness, the contraction ratio β is the main factor which affects dimensionless backflow region length l_b. The empirical expression, by means of the numerical simulation results from Fig. 6, could be obtained:

$$l_b = -5.0718(a)^{-0.1724}\beta^2 + (-10.432a + 4.6662)\beta + 6.1257(a)^2 - 1.5293a + 3.276 \quad (10)$$

This expression is valid for $\beta = 0.4 - 0.8$, $\alpha = 0.05\text{-}0.25$ and $Re>10^5$.

CONCLUSION

For an orifice plate energy dissipater, its dimensionless backflow region length l_b after this orifice plate is the function of the contraction ratio of the orifice plate β, the ratio of the orifice plate thickness α. And the effects of Re could be neglected on the l_b when this number is larger than 10^5.The contraction ratio β is the key factor that dominates the dimensionless backflow region length l_b. The less the contraction ratio β is, the bigger is the dimensionless backflow region length l_b. The relationship of l_b, β and α could be expressed as Eq. 10 and can provide reference for arranging the distance between two orifice plates in installing multi-stage orifice plates.

REFERENCES

Zhou, J.P., Z.Y. Yang and G.F. Chen, 2006. Status and challenges of high dam in China. J. Hydraulic Eng., 37: 1433-1438.

Zhang, Z.H., R.P. Wang and Y.Z. Wang, 1991. A general review on the layout of hydro-junction and technique of flood discharge and energy dissipation for high dams in China. J. Water Resour. Water Eng., 2: 1-15.

Lin, B.N., 1985. Reviews on energy dissipation technologies for high-speed flows in China. J. Hydraulic Eng., 5: 23-26.

Wu, J.H., G.C. Chai and T. Xiang, 1995. Hydraulic characteristics and optimization of orifice plate discharge tunnel of the Xiaolangdi hydropower project. J. Hydraulic Eng., 5: 101-109.

Ai, W.Z. and T.M. Ding, 2010. Orifice plate cavitation mechanism and its influencing factors. J. Water Sci. Eng., 3: 321-330.

Ball, J.W., T. Stripling and J.P. Tullis, 1975. Predicting cavitation in sudden enlargements. J. Hydraulics Division, 101: 857-870.

He, N. and Z.X. Zhao, 2010. Theoretical and numerical study of hydraulic characteristics of orifice energy dissipator. J. Water Sci. Eng., 3: 190-199.

Wang, D.C. and P.J. Yue, 1987. An experimental studies on energy dissipation of orifice plate in tube. J. Hydrodynamics Ser. A, 2: 41-50.

Zhao, H.Q., 1993. Discussion on multi-orifice plate energy dissipation coefficient. J. Water Conservancy Hydropower Technol., 6: 45-50.

Wu, J.H., W.Z. Ai and Q. Zhou, 2010. Head loss coefficient of orifice plate energy dissipator. J. Hydraulic Res., 48: 526-530.

Yang, Y.Q. and H.H. Zhao, 1992. Numerical simulation of turbulent flows passed through an orifice energy dissipator within a flood discharge tunnel. J. Hydrodyn. Ser. B, 4: 27-33.

Xia, Q.F. and H.G. Ni, 2003. Numerical simulation of plug energy dissipater. J. Hydraulic Eng., 8: 37-42.